Received: 21 September 2023 | Revised: 22 January 2024 | Accepted: 22 January 2024

DOI: 10.1111/jeu.13021

Journal of Eukaryotic Microbiology | ISOP Published by the International Society of Protistologists

ORIGINAL ARTICLE

Identification of a new gregarine parasite associated with mass mortality events of freshwater pearl mussels (*Margaritifera margaritifera*) in Sweden

Anders Alfjorden[1,2] | **Ioana Onut-Brännström**[3,4] | **Niklas Wengström**[5,6] | **Arni Kristmundsson**[7] | **Mahwash Jamy**[1] | **B. David Persson**[2] | **Fabien Burki**[1,8]

[1]Department of Organismal Biology, Program in Systematic Biology, Uppsala University, Uppsala, Sweden

[2]Department of Animal Health and Antimicrobial Strategies, National Veterinary Institute (SVA), Uppsala, Sweden

[3]Department of Ecology and Genetics, Evolutionary Biology Center, Uppsala University, Uppsala, Sweden

[4]Natural History Museum, University of Oslo, Oslo, Norway

[5]Swedish Anglers Association, Gothenburg, Sweden

[6]Department of Biological and Environmental Sciences, University of Gothenburg, Gothenburg, Sweden

[7]Institute for Experimental Pathology at Keldur, University of Iceland, Reykjavik, Iceland

[8]Science for Life Laboratory, Uppsala University, Uppsala, Sweden

Correspondence
Anders Alfjorden and Fabien Burki, Department of Organismal Biology, Program in Systematic Biology, Uppsala University, Norbyvägen 18D, 752 36 Uppsala, Sweden.
Email: anders.alfjorden@ebc.uu.se and fabien.burki@ebc.uu.se

Funding information
SciLifeLab, a Formas Future Research Leader grant, Grant/Award Number: 2017-01197; Swedish Research Council, Grant/Award Number: 2018-0597 and 2017-04563

Abstract

Freshwater bivalves play key ecological roles in lakes and rivers, largely contributing to healthy ecosystems. The freshwater pearl mussel, *Margaritifera margaritifera*, is found in Europe and on the East coast of North America. Once common in oxygenated streams, *M. margaritifera* is rapidly declining and consequently assessed as a threatened species worldwide. Deterioration of water quality has been considered the main factor for the mass mortality events affecting this species. Yet, the role of parasitic infections has not been investigated. Here, we report the discovery of three novel protist lineages found in Swedish populations of *M. margaritifera* belonging to one of the terrestrial groups of gregarines (Eugregarinorida, Apicomplexa). These lineages are closely related–but clearly separated–from the tadpole parasite *Nematopsis temporariae*. In one lineage, which is specifically associated with mortality events of *M. margaritifera*, we found cysts containing single vermiform zoites in the gills and other organs of diseased individuals using microscopy and in situ hybridization. This represents the first report of a parasitic infection in *M. margaritifera* that may be linked to the decline of this mussel species. We propose a tentative life cycle with the distribution of different developmental stages and potential exit from the host into the environment.

KEYWORDS
freshwater perl mussel, gregarine, ISH, *Margaritifera margaritifera*, mass mortality, mortality, Nematopsis, pathology, phylogeny, TEM

INTRODUCTION

A large diversity of protistan parasites is known to affect invertebrate hosts. In marine environments, it is well established that mortalities in bivalve populations (e.g. mussels, oysters, clams, cockles, and scallops), either in wild populations or in aquaculture, are often caused by different groups of parasites belonging to Apicomplexa,

Perkinsea or Ascetosporea (Bower et al., 1997; Carnegie et al., 2003; Carrasco et al., 2015; Čižmek et al., 2020; Kristmundsson & Freeman, 2018). In comparison, much less is known from freshwater systems, even though populations of different mussel species have been declining (Aldridge et al., 2023; Haag, 2019; Richard et al., 2020). The decline among different species of freshwater mussels has mainly been explained by the degradation of water quality caused by anthropogenic activities such as dredging, sedimentation, land-originating run-offs, eutrophication, and coal mining (Haag, 2019; Richard et al., 2020). However, the possibility of infectious agents, such as protistan parasites, has generally not been considered.

The freshwater pearl mussel *Margaritifera margaritifera* inhabits rivers and creeks throughout the northern Holarctic region, which includes populations from North America (common name in the US and Canada: eastern pearlshell) as well as northern Europe. While other freshwater mussel species have a wide tolerance for different aquatic environments, *M. margaritifera* only lives in highly oxygenated streams with clear running water, which makes it particularly vulnerable to fluctuations in environmental conditions (Henrikson & Söderberg, 2020; von Proschwitz & Wengström, 2021). Indeed, this species is assessed as globally threatened according to the International Union for Conservation of Nature (IUCN) Red List (Moorkens et al., 2017), while in Sweden it is highly endangered (Westling et al., 2020). Currently, only one third of the Swedish populations is considered healthy with reproducing populations (Henrikson & Söderberg, 2020; von Proschwitz & Wengström, 2021).

Swedish populations of *M. margaritifera* have been closely monitored due to their critical status, with an overview of mortality events including some microscopic as well as macroscopic descriptions performed in 2016 and 2017 (Wengström et al., 2019). From populations experiencing mass mortality events (MME), patterns of pathological changes in gonads, foot, digestive gland and mantel are described. However, no clear conclusion on the etiology or possible causes for the observations and histopathological changes could be drawn (Wengström et al., 2019). In the Swedish locality of Teåkersälven, where new MME were detected in 2017, we collected a few moribund mussels and performed initial histopathology, which revealed the presence of cysts with similarities to gregarines (Apicomplexa).

Gregarines are a group of protists infecting almost exclusively invertebrate hosts. They are highly diversified, both morphologically and genetically (Cavalier-Smith, 2014; Clopton, 2002; Leander, 2008; Rueckert et al., 2011). However, there is no published report of gregarines in *M. margarifera* nor any other freshwater mussels, and more generally, to our knowledge, no published data are available on apicomplexan parasites in freshwater mollusks. In contrast, several studies have shown that gregarines are common parasites in marine bivalves (Azevedo & Padovan, 2004; Belafastova, 1996; Berrilli et al., 2000; Hatt, 1931; Kinne & Lauckner, 1983; Silva et al., 2019; Tuntiwaranuruk et al., 2004; Vivares, 1969). Marine gregarines are also common in other invertebrates such as crustaceans and polychaetes as well as the vertebrate group of tunicates (Iritani et al., 2021; Rueckert et al., 2011; Wakeman, 2020) and probably also common in arthropods and annelids in freshwater systems, where they are known to infect a variety of insects that live part of there life in aquatic environments (Clopton, 2002, 2009; Clopton et al., 2007; Lantova & Volf, 2014; Smith & Cook, 2012; Smith-Herron, 2015; Tseng, 2007). Tadpoles have also been shown to host a gregarine species, which was described as *Nematopsis temporariae* belonging to Eugregarinorida (terrestrial clade I) based on microscopy, ultrastructure, and 18S rDNA phylogenetic analysis (Chambouvet et al., 2016). However, the description of a *Nematopsis* species in a terrestrial group of gregarines is inconsistent with existing taxonomy, considering this genus as part of the marine clade Porosporidae (Cavalier-Smith, 2014; Rueckert et al., 2011). Thus, the affiliation of the tadpole parasite to *Nematopsis* should be considered unresolved.

To investigate the gregarine-like parasite observed in *M. margaritifera*, we collected specimens at several time points over 3 years in Teåkersälven experiencing MME, as well as in a reference healthy population (from the locality Stommebäcken). DNA sequencing of the small subunit of the ribosomal DNA (18S rDNA) revealed a novel diversity of gregarines related to the tadpole parasite *N. temporariae* (Chambouvet et al., 2016). Histology, in situ hybridization (ISH), and transmission electron microscopy (TEM) on specimens collected from Teåkersälven provide the first report of a parasitic infection, including a putative lifecycle, in the endangered *M. margaritifera*, and more generally the first report of gregarines in freshwater mollusks.

MATERIALS AND METHODS

Sample collection

Live specimens of *M. margaritifera* were collected in two close rivers from Sweden: Stommebäcken (N 58.7512057, E 12.2262805) and Teåkersälven upstream, purification site (PS): (N 58.7572073, E 12.2311112) and downstream, (PS): (N 58.7572073, E 12.2311112). Teåkersälven has been experiencing ongoing mortalities (MME) and a rapid decline since 2016. Data summarizing population sizes of both streams are listed in Table S1, clearly showing this decline between 2016 and 2019. The animals collected in Teåkersälven were showing signs of poor health (i.e. laying on top of the substrate, gaping, and a slow response to tactile stimuli (Richard et al., 2020)). Sampling from the

MME population was performed in September 2018 (5 specimens collected), October 2019 (10 specimens collected), and June 2020 (20 specimens collected), while the healthy reference population at Stommebäcken (no signs of mortalities were observed) was sampled in September 2018 (3 specimens collected), and June 2020 (10 specimens collected). A bathyscope was used to identify the mussel individuals. A permission for collecting limited numbers of freshwater pearl mussels was granted for this study by the regional authority (länssstyrelsen Västra Götaland: 623-28113-2018; 623-37022-2019; 621-22570-2020). The mussels collected in 2018 and 2020 were transported in containers with water from the sampling sites to the National Veterinary Institute (SVA, Uppsala, Sweden), and kept cold during transport using cooling blocks. The mussels collected in 2019 were directly preserved at the sampling site using 96% ethanol. In the lab, these animals were dissected in 2–3 mm thin cross-sections covering the digestive gland region, cut longitudinally in two halves, and stored in 96% ethanol for subsequent DNA extraction.

Macroscopic observations

Macroscopic investigations were made as described in Wengström et al. (2019) and observations are listed in Table S2. Specimens collected in 2018 and 2020 were screened for uncharacteristic gross morphological anatomy and biological measures were taken (Table S2), while animals from 2019 were only investigated by molecular methods. Before fixation, released fluid and cells from sectioned organs were collected for cytology by tissue imprints and PCR by cotton swabs. The swabs were directly frozen and stored at −20°C until DNA extraction.

Histology, cytology, and transmission electron microscopy

Two parallel cross-sections were collected in tandem cuttings to include both digestive gland and gonads from each animal from the MME population (2018, $n=5$; 2020, $n=20$) and fixed in Davidssons freshwater fixative for 48 h. Fixed sections were further processed according to routine histological protocols (Howard & Smith, 1983) and stained by hematoxylin and eosin (HE). Cytological imprints were stored dry and dark until further processing and stained using Hemocolor rapid stain of blood smears (product number 1.11956, Merck KGaA, Darmstadt, Germany).

Stained sections of each sampled specimen were inspected by microscopy using both low-power (Olympus SZ binocular stereo zoom microscope; Tokyo, Japan) and high-power magnification (Nikon Labophot; Tokyo, Japan). Photos were taken with a Canon EOS 500D attached to a microscope by a lens-adaptor (Martin Microscope Company MM-SLR adaptor S/N:0468; Easley, SC USA). Additional photos were taken for illustration of the putative life cycle, using an inverted microscope Nikon eclipse Ts2R using Nikon Plan Fluor DIC, 100X/1.30 oil lens, and TIS Camera USB 3.0 Monochrome 1/1.2 CMOS.

Organ biopsies for TEM were collected from the digestive gland and fixed in 2.5% glutaraldehyde solution (0.1 M Phosphate Buffer, pH 7.4 (PB)). Selected samples (2018, $n=2$; 2020, $n=2$) were further processed by PB rinsing before and after 1 h of incubation in 1% osmium tetroxide and then dehydrated in graded alcohols (70%–99.9%), followed by incubation in propylene oxide for 5 min. Embedding followed routine protocol, using Epon Resin and propylene oxide (1:1) for 1 h, two changes of 100% resin, and subsequently polymerization in Epon Resin for 2 days. Semithin sections (1–2 μm) were stained with toluidine blue and examined for areas of interest. The block was trimmed and ultrathin sections (60–70 nm) were cut in a Leica UC7 Ultramicrotome and placed on a grid. Sections were contrasted using 5% uranyl acetate for 10 min and 3% Reynolds lead citrate for 2 min. Grids were examined by TEM (FEI Tecnai G2) operated at 80 kV.

DNA extraction and PCR amplification

For the ethanol-preserved animal specimens, the ethanol was evaporated for 10 min and rinsed for 30 min in 1× PBS solution before the DNA isolation procedure. To break the cell wall of encysted cells and increase the DNA yield, all samples collected from digestive glands were pretreated using freeze–thawing cycles (3× 10 min deep freezing at −70°C followed by 1 min heat block treatment at 90°C) and digested with Proteinase K and ATL buffer at 56°C overnight under slow shaking condition (60 rpm). DNA was isolated with Qiagen DNeasy Blood and tissue kit, following the manufacturer's instructions. DNA concentration was measured on a Qubit Fluorometric Quantification Machine (Thermo Fisher Scientific).

The 18S rDNA sequences were obtained in two steps. First, DNA was amplified from all mussels collected in 2018 ($n=8$) using a general nonmetazoan reverse primer 18s-Euk 1134-R (5′-TTTAAGTTTCAGCCTTGC-3′) (Bower et al., 2004; Del Campo et al., 2019) combined with the primer Int F1 (5′-GATTAAGCCATGCATGTCTAAG-3′) known to amplify marine gregarines (Wakeman & Leander, 2013). The PCR reaction was conducted using EconoTaq PLUS 2× Master mix (Cat no. 30035-1, Lucigen, LGC Biosearch technologies, USA) as follows: Initiation, 94°C for 2 min; 35 cycles of 94°C for 30 s, 52°C for 1 min, 72°C for 1.5 min; final extension, 72°C for 10 min. PCR products were cloned using

StrataClone PCR cloning kit (product no: 240205, Agilent Technologies Sweden AB, Kista) and re-amplified with M13F/M13R primers using DreamtTaq (Thermo Fisher Scientific, Baltics UAB, Vilnius, Lithuania). Bands of the expected size were purified with Illustra™ ExoProStar™ 1-step Enzymatic PCR and Sequence reaction clean up Kit (prod no. US77702, GE Health Care UK Limited, Buckinghamshire). Purified clones were Sanger-sequenced in both directions at Macrogen (Macrogen Europe BV, Amsterdam, Netherlands). The sequences were verified, trimmed, and assembled with Geneious v.9 (Kearse et al., 2012). Based on these initial sequences, new specific primers were designed to further explore the *Nematopsis* lineage diversity, on mussels sampled ($n = 48$) between 2018 and 2020. Primers were designed to cover the v4 region but also to reach almost full length of 18S rDNA using both available NCBI sequences from tadpoles (Chambouvet et al., 2016) and with the initial sequences generated in this study (above). All primers used in our study are listed in Table S3.

All gregarine 18S rDNA sequences obtained in this study have been deposited in GenBank under the accession numbers (OR133332–OR133340, OR167014–OR167032, OR167182–OR167194, OR167380–OR167381, OR168121–OR168122, OR168627). The accession numbers of the sequences are listed in Table S4.

Environmental diversity

To investigate the environmental phylogenetic diversity of *Nematopsis*, we BLASTed (Altschul et al., 1990) the Sanger sequences against a long-read environmental dataset previously published (Jamy et al., 2022), using a 90% similarity cut-off. Briefly, this dataset was generated by PacBio sequencing of ~4500 bp of the ribosomal operon (18S, ITS1, 5.8S, ITS2, 28S) of the eukaryotic community from various habitats, including four freshwater samples. Three samples were obtained from Swedish lakes (Lake Erken, Lake Ersjön, and Lake Stortjärn) (Jamy et al., 2022) while three samples was collected from permafrost thaw ponds from Canada (Peura et al., 2020) (Table S5). We also analyzed short-read environmental data to investigate the distribution of *Nematopsis* in various habitats using datasets corresponding to Tara Oceans (de Vargas et al., 2015; V9), VAMPs (Huse et al., 2014; V9), Scandinavian Lakes (Khomich et al., 2017; V4), Neotropical soils (Mahé et al., 2017; V4), Global soils (Bates et al., 2013; V4), Swiss alpine soils (Seppey et al., 2020; V4 and Singer et al., 2020; V9), Lake Baikal (Annenkova et al., 2020; V4), and St. Charles River (Cruaud et al., 2019; V4). All datasets were cleaned and Amplicon Sequence Variants (ASVs) were generated using DADA2 (Callahan et al., 2016). Sanger sequences and positive hits from the long-read dataset were used to query the ASVs with BLAST (85% similarity threshold), using the V4 and V9 fragments as appropriate (Altschul et al., 1990).

Phylogenetic analysis

The 18S rDNA sequences obtained from MME and reference populations of *M. margaritifera* were blasted online against the NCBI nucleotide database (last access: May 2023) and representative hits across Apicomplexan diversity, plus publicly available environmental sequences were retrieved. Additionally, reference sequences from all the major Apicomplexan lineages and Chrompodellida were included in the dataset together with Perkinsozoa and Dinophycaea, chosen as outgroup. The OTUs assembled from the long-read environmental sequences described in (Jamy et al., 2022) were also added to the final dataset (see section above). A list of all sequences used for phylogenetic analyses is provided in Table S6. The sequences were aligned with MAFFT v.7.407 (Rozewicki et al., 2019) using the mafft-linsi algorithm. TrimAl v. 1.4.1 (Capella-Gutiérrez et al., 2009) with gappyout setting was used to trim ambiguously aligned sites. IQTREE v.2.0 -rc2-omp-mpi (Minh et al., 2020) was used to infer a maximum likelihood (ML) tree, using the best-fitting model of nucleotide substitutions GTR + F + I + G4 as determined by the corrected akaike information criterion. The branch support was assessed with standard nonparametric bootstrap based on 100 bootstrap replicates. The raw, aligned, and trimmed fasta files used for the phylogenetic analysis are available in FigShare: 10.6084/m9.figshare.25053401.

In situ hybridization (ISH)

We followed the method described in (Kristmundsson & Freeman, 2018), with one modification using an extra blocking step against endogenous biotin signal. Two biotin labeled probes: 360rev(ISH) 5′-TGGACTGTTGCCAGTCCTTC-Bio and 1143rev(ISH) 5′-TAGACGTATGATTGACGTGC-Bio were designed to specifically target the new gregarine sequences amplified from the MME population of *M. margaritifera* (Teåkersälven) using sequences originating from mussels collected in 2018, i.e. lineage A. Cross-sections from embedded mussels in paraffin blocks were cut at 7 µm and 5 µm thickness, then deparaffinized, rehydrated in distilled H_2O followed by PBS incubation and permeabilized for 12 min at 37°C using 7 µg/mL proteinase K in Tris-buffered saline (TBS) pH 8, followed by washing in PBS. The sections were then incubated in 0.4% paraformaldehyde in PBS for 15 min followed by washing with distilled water. To prevent unspecific binding, we used a streptavidin-biotin blocking kit (Vector Laboratories Inc., Burlingame, USA) by first incubating with streptavidin for 15 min, washing in buffer followed by 15 min

incubation with biotin, and washing. This was followed by a secondary blocking of hydrogen peroxide, where 0.3% hydrogen-methanol was added for 10 min followed by a 5-min washing step repeated one time. The hybridization buffer was added with probes using Frame-Seal™ enclosure (Bio-Rad, Sundbyberg, Sweden). By adding 100–120 μL of ready-to-use hybridization buffer (Roche prod Merck KGaA, Darmstadt, Germany) mixed with both probes (2.25 ng/mL of each), the sections were sealed, denatured at 95°C during 4 min and hybridized at 45°C for 8 h (overnight) in a humid chamber. Negative control slides were incubated in buffer without adding the probes. The hybridization buffer was washed off in two steps with non-stringent and stringent buffer, respectively: first with 2× SSC kept at room temperature followed by second buffer SSC with 0.1% Tween 20 stored at 45°C (saline-sodium citrate buffer, SSC). For signal detection, the samples were incubated with horseradish peroxidase-labeled streptavidin (Dako, Agilent Technologies, Glostrup, Denmark) for 20 min at room temperature followed by 3 × 5 min washing in PBS (pH 7.4) and then adding Nova Red Peroxide substrate for 10 min (Vector laboratories Inc., Burlingame, USA, Maravai Life Sciences). Hematoxylin was used as counterstain followed by dehydration and mounting of coverglas.

RESULTS

Phylogenetic analysis reveals three novel terrestrial gregarine lineages isolated from *Margaritifera margaritifera*

After a mass mortality event (MME) of *M. margaritifera* in Teåkersälven first detected in 2017, a general decline in the population was continuously observed (Wengström et al., 2019), culminating at about 65% in 2019 (Table S1). To determine the potential role of a parasitic infection in this decline, specimens were collected between 2018 and 2020 from both the MME population (35 specimens collected) and a healthy reference population in a nearby locality (Stommebäcken, 13 specimens collected). A total of 46 sequences were obtained using 18S rDNA primers known to amplify gregarine diversity (see Material and Methods and Table S4). To investigate the phylogenetic origin of these sequences, a diverse set of apicomplexan homologs were retrieved by BLAST against the NCBI database, as well as six long-read environmental sequences obtained from (Jamy et al., 2022) (Table S5). Only one short-read metabarcoding sequence was identified by our search against various datasets corresponding to a rare OTU from a Norwegian lake (Khomich et al., 2017); because this short sequence was identical to two of the long reads (isolated from Swedish lakes), we did not include it in the phylogenetic reconstruction.

Maximum Likelihood (ML) phylogeny showed that all new sequences isolated from *M. margaritifera* are part of the terrestrial clade 1 of gregarines, together with neogregarines, monocystids, and species from insects especially those associated with water (e.g. damselfly, dragonfly, water scorpion) and other environmental sequences (Figure 1, Figure S1). The newly generated sequences form three distinct lineages, here tentatively named lineages A-C (Figure 1). Lineage A is supported by 99% bootstrap and includes the majority of sequences isolated from the MME population (35/36), one sequence isolated from the reference populations, and five long-read environmental sequences from permafrost soil from Canada and Swedish lakes and bogs (Figure 1, Figure S1). Lineage A branches together (bootstrap support = 100%) with a clade comprising the previously published sequences of the tadpole parasite *Nematopsis temporariae* (Chambouvet et al., 2016) and an environmental sequence from the Canadian permafrost soil, but also with a distinct sequence (lineage B) isolated from the 2019 MME population in Teåkersälven (Figure 1, Figure S1). Our phylogenetic analysis also identified a third and novel gregarine clade (lineage C) that is weakly associated (bootstrap support = 63%) with the group comprising lineages A, B, and *N. temporariae*. Sequences from lineage C were only identified in *M. margaritifera* individuals collected from the healthy reference population at Stommebäcken (Figure 1, Figure S1).

Lesions in *Margaritifera margaritifera* tissues collected in MME

External inspection of specimens collected in the MME population from Teåkersälven revealed thickening and whitening of the mantel and reductions in gonads (Figure S2A). Upon gross morphological investigation, no gonads were visible in the 2018 samples. In 2020, only 1/20 specimens (5%) showed gonads detectable by eye (Figure S2B,C). Macroscopic observations of the digestive system, foot, connective tissue, and muscle layers did not show any clear signs of discoloration or emaciation (Table S2).

Closer histological examinations revealed several lesions in the mantel, gills, digestive glands, and gonads. In addition, patterns of increased hemolymph infiltration within connective tissue were found in the mantel (Figure 2A), likely expanding its thickness. The hemolymph regions of the mantel were highly infiltrated by hemocytes in 4/5 mussels collected in September 2018, migrating from blood sinuses into connective tissue and the hemolymph-rich areas (Figure 2B). The hemocytes were hypertrophied or irregularly shaped often with a dislocated nucleus, enclosing weakly stained or brown structures (indicated with white and blue arrowheads in Figure 2B). A similar pattern was seen in many hemocytes or phagocytic cells within the auricles of the heart (Figure 2C). These enlarged phagocytic cells reached 11.3 μm ($n = 4$, stdev = 0.79) in the mantel

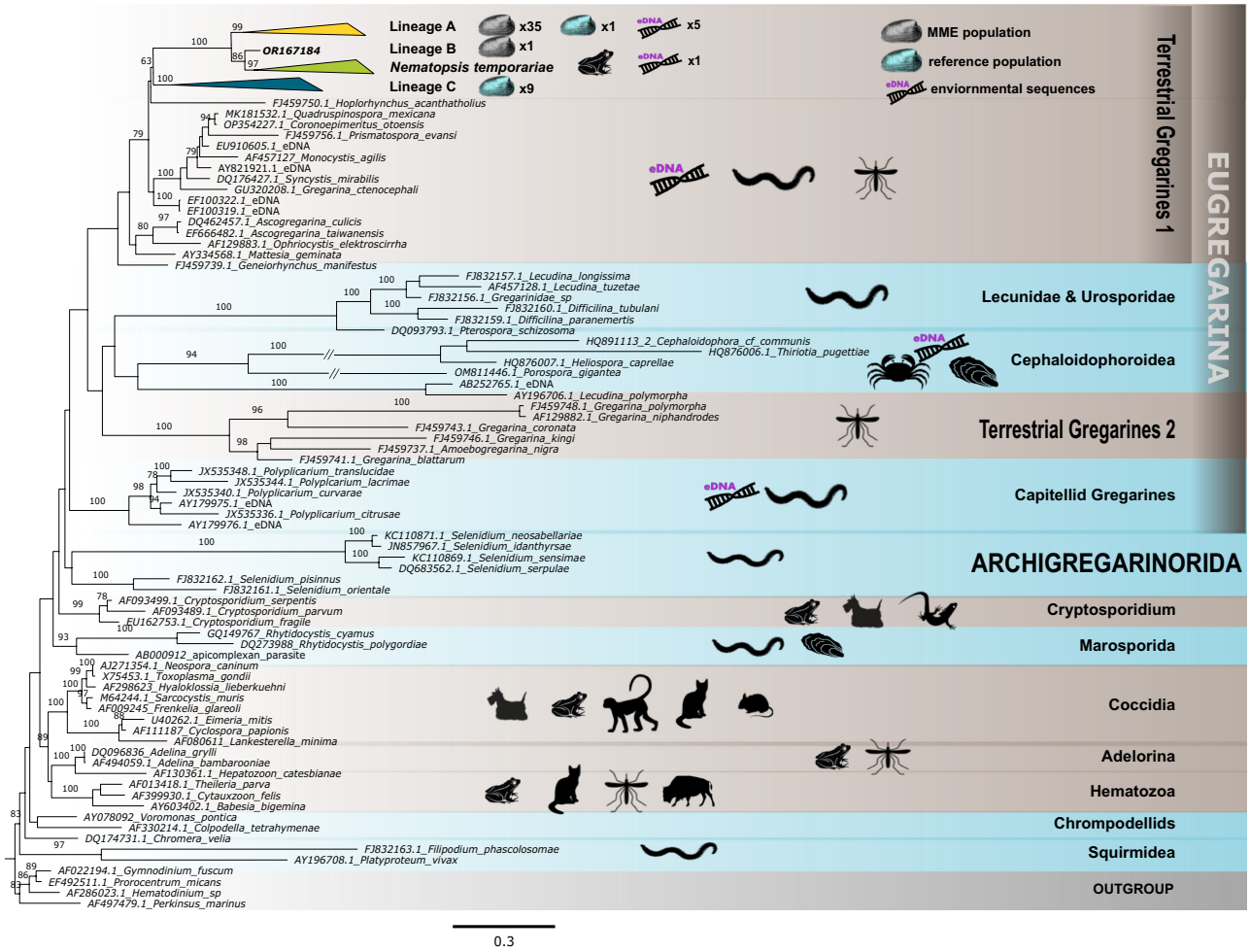

FIGURE 1 Maximum likelihood (ML) phylogenetic tree based on the 18S rDNA gene with placement of the newly produced gregarine sequences isolated from MME and reference populations of *Margaritifera margaritifera*. The number on branches is bootstrap support based on 100 replicates (bootstrap support below 70% is not shown). For all NCBI sequences, the GenBank accession number and the taxon name are listed. The double slashed line represents manually shortened branches for fitting purposes. Known hosts and environmental sequences are shown using pictograms. The tree was rooted with four sequences belonging to Perkinsozoa and Dinophyceae as outgroups. Lineages A, C, and the *N. temporariaea* clade were collapsed for clarity but their full version is available in Figure S1. The scale bar represents the estimated number of substitutions/sites.

and 13.4 μm (n = 9, stdev = 0.97) in the heart. Cellular infiltration or hyperplasia within gills and mantel was observed forming basophilic clustering of cells within or attached to skeletal parts of the gills as well as in hemolymph gill sinuses and within connective tissue Figure 2D–F).

Degenerative changes were also observed within the digestive gland, primarily in September 2018. All

FIGURE 2 Histopathological lesions associated with gregarine infiltration of mussels collected from the MME population. (A) Infiltration of hemolymph (basophilic droplets) and hemocytes, within the connective tissue of the mantel. (B) Enlarged area (marked as white square in A), showing diffuse hemolymph spread within connective tissue (blue arrowhead) and invasion of hemocytes (white arrowhead). Note that some hemocyte-nuclei are displaced indicating phagocytized material within cytoplasm (blue arrowhead). (C) Large phagocytic cells within heart auricles, enclosing multiple pigmented granules or micro-cells. (D) Clusters of basophilic cells expanding from the gill filaments, chitinous skeleton part. (E) Close-up of the hyperplasia (marked as a white square in D), where the basophilic cells are characterized by thick cell walls developing within host epithelia of the gill. Host nuclei are indicated with a yellow arrow. (F) Gill vessels or sinuses, are infiltrated with large and thick-walled basophilic spheres. Signs of cell division are indicated by blue arrows. (G) Large numbers of vacuoles develop within the digestive gland epithelia, enclosing weakly eosinophilic or basophilic cells. (H) Parasitic vacuoles within the vesicular cells (VC) are visualized by phase contrast (arrow). (I) The spherical cells within the vacuoles indicated different origins, enclosing both detachment of basophilic cells (blue arrowhead) and cyst formation within eosinophilic vesicular cells (white arrowhead). (J) Gonad follicles enclosing normal oocytes. (K) Ovary follicles are filled with developing oocytes as well as pycnotic and degenerative cells (blue arrowhead). Increased numbers of pigmented granules. (L) Gonad follicle without signs of gonad development. Follicles filled with brown degenerative matter or cell debris potentially due to the oocyte resorption process.

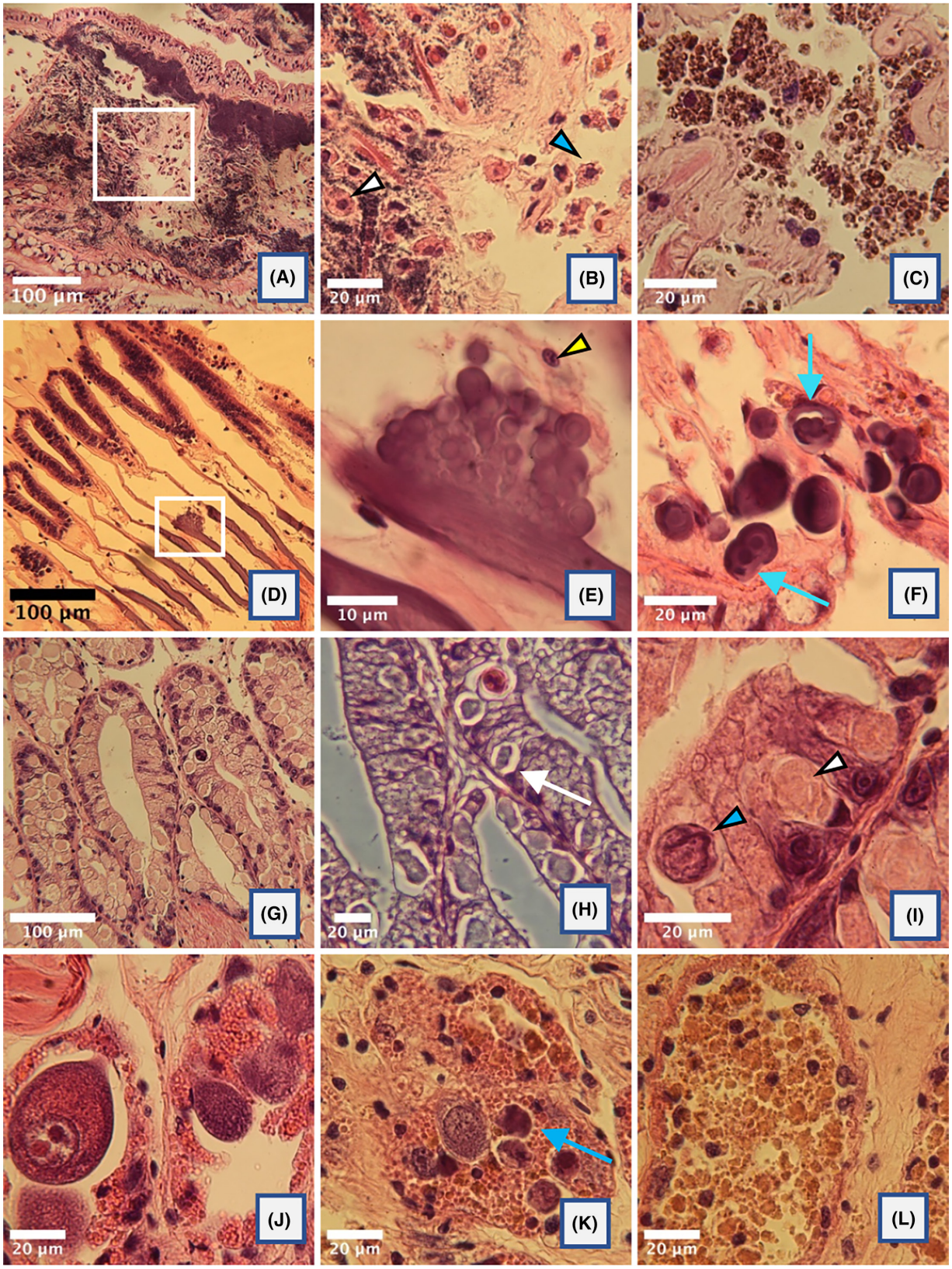

five mussels collected from the MME population exhibited extensive signs of vacuolization, affecting over 50% of the cells (Figure 2G,H). Epithelial lysis, necrosis or disintegration caused the detachment of many cells from basal layers, releasing cells or cell content into the lumen of the digestive glands. This affected both vesicular and basophilic cells within tertiary gland ducts (Figure 2I). Minor changes and much

less vacuolization were observed in June, where 11 out of 20 mussels showed signs of vacuolization and in much lower numbers (less than 10 cells/section). Finally, most gonads exhibited impaired development with reduced or absence of normal cells. In the MME population, only one specimen had regular oocytes (Figure 2J), while many ovaries showed signs of atrophy with cells appearing pyknotic and densely basophilic (Figure 2K). Among mussels collected in June, 17 out of 20 specimens had completely depleted gonad cells, with follicles containing cellular debris instead (Figure 2L). These degenerative changes could also be related to resorption due to the reuse of oocytes after the spawning period.

Putative infiltration of a new gregarine parasite

To explore the potential link between the lesions described above caused by invading cells in different tissues and the new sequences obtained, in situ hybridization (ISH) was utilized with probes specifically designed to target the isolates of lineage A. Mussels collected in 2018 and 2020 in Teåkersälven (two specimens for each year) revealed gregarine cells in the hemolymph compartment and gills as well as within digestive gland. Mono or dizoic cysts were observed in hemolymph sinuses in the mantel (Figure 3A,B). In the skeletal part of the gill, zoites were forming mono-, di- or polyzoic cysts, and were attached to the endothelium of the gill vessels (Figure 3C–E). A systemic spread and low numbers of monozoic thick-walled, histozoic sporocysts were detected embedded in other organs such as the digestive gland (Figure 3F). Free zoites were also detected within the lumen of the tertiary digestive glands (Figure 3G), indicating oral uptake of detached cells from the mantel and gills (Figure S3D and S3E). Within digestive glands, invading zoites were observed attaching to the surface of epithelial cells of tubuli, as well as proliferating within the tubular epithelia, migrating deep within the digestive gland. These infiltrating zoites gave a strong positive ISH staining in June (Figure 3H,I), but larger sporoblast containing immature oocyst stages within the digestive gland gave a weaker signal (Figure 3J,K), and only weak or no signal were recovered from September 2018.

Developmental forms of the new parasite

Light microscopy revealed eosinophilic but weakly stained zoites within the hemocytes circulating through the mantel, gills, and heart, sometimes dislocating the host cell nucleus (Figure 4A,B). Large numbers of small round or vermiform cells were also seen within hemocytes in the heart's auricles, presumably due to phagocytosis (Figure 4C). These cells might correspond to invading naked gregarine infiltrating cells, for example, similar to gymnospores known to infect marine bivalves (Prytherch, 1940). The intracellular circular spores exhibited considerable variation in size and shape, with a mean diameter of 3.06 µm (n = 20, stdev = 0.75).

The hemolymph was distributed as strongly basophilic droplets, which were infiltrated with polymorphic zoites enclosed in transparent spheres in both the mantel and gills. Single or double vermiform stages, measuring approximately 2–15 µm in length, were folded into open semicircles or closing full circles within these spheres (Figure 4D). In addition, mono/dizoic thick-walled cysts were enclosed in connective tissue, as histozoic cysts of the gills and mantel as well as freely dispersed within the hemolymph compartment (Figures 2E,F, 4E,F), morphologically corresponding to the cells observed by ISH (Figure 3A–E). The examination of the mantel and gills revealed signs of epithelial loss, as well as the release of hemocytes and sporoblast-like cells (Figure 4G). Similar cells were observed infiltrating the digestive gland indicating an oral route via the stomach and further to the tubuli channels. Multiple such cells were seen entering the digestive glands through digestive tubules, an observation also supported by ISH (Figure 3G).

The pattern of vacuoles forming within the digestive gland of the mussels from the MME population was further investigated by light microscopy. Phase contrast showed the formation of parasitophorous vacuoles where pairs of zoites (presumably zygote or syzygy formation) developed into sporoblasts enclosing oocysts with inner sporocysts (Figure 4H,I). These oocysts, reaching over 20 µm in size (Figure 4I), enclosed two inner sporocysts without clear signs of inner sporozoites, that is, unsporulates oocysts. Two types of larger vermiform parasite cells, basophilic and eosinophilic, were also observed in front-to-front position, which we interpret as merging gamonts in a process termed syzygy, indicating a gregarine gamogonial phase. From ruptured parts of the digestive glands, immature sporocysts as well as mature disporous ones were also found (Figure 4J).

The majority of the oocysts were released unsporulated, thus the intestine was also investigated to follow the potential release of parasites as a fecal outlet. The intestinal lumen contained multiple sporocysts, suggesting a link between immature sporozoites (sporoblasts) and oocysts that could have developed into free sporocysts during the release. These undifferentiated sporocysts with a mean diameter of 14.5 × 13.9 µm (n = 5) are likely also divided further into two parts as seen in Figure 3K. Two types of cysts showed large variations in size and shape: smaller cysts (Figure 4K) with a mean diameter of 9.75 × 9.0 µm (n = 22, range 6.8–11.2 µm), and larger thick-walled cysts with a diameter of 21.7 × 21.2 µm (n = 1) (Figure 4L). Since no fecal samples were investigated directly upon sampling, the final morphology of sporulated sporocysts is unresolved, even though the double, thick, and refringent

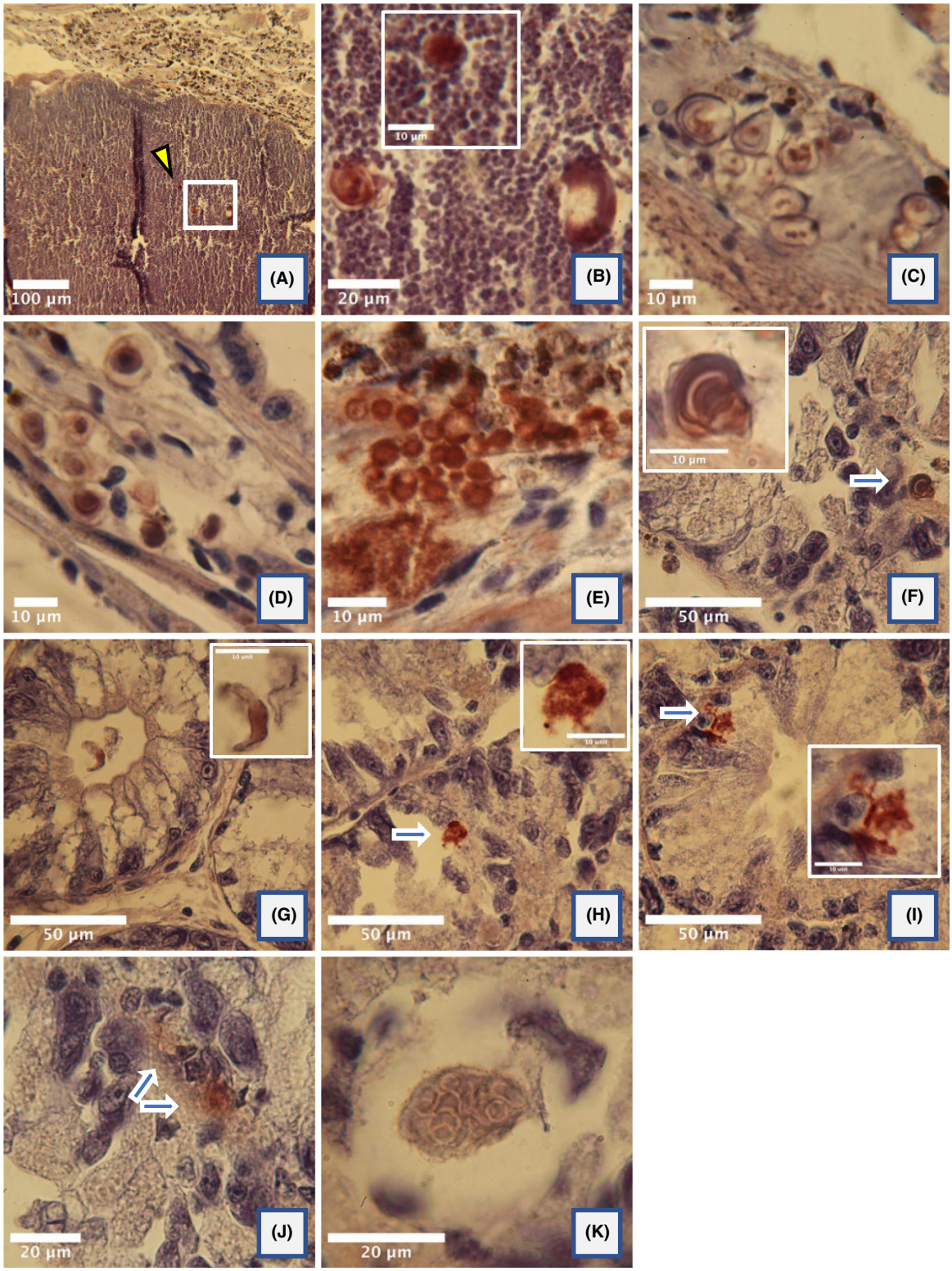

FIGURE 3 In situ hybridization of lineage A cells showing different development stages in *Margaritifera margaritifera* from Teåkersälven. Images A–D are from specimens collected in September 2018, and images E–K are from specimens collected in June 2020. (A and B) Positive reaction (Nova Red, avidin-biotin complex) in dorsal hemolymph sinuses, adjacent to heart auricles, visualizing circulating zoites. (C) Developing zoites embedded within gill skeleton parts. (D and E) Gill sections showing multiple crescent folded zoites infiltrating epithelial layers. (F) Section of digestive glands showing a single histozoic cyst embedded between the digestive glands, adjacent or within capillary vessels. (G) Infiltrating zoites within the lumen of digestive glands. (H and I) Invasion of zoites attaching to and infiltrating vesicular cells. (J) Early sporogony development, zygote or sporoblast deeply embedded within digestive gland cells. (K) Multicellular sporoblast, within the parasitic vacuole, enclosing multiple sporogonic developmental stages.

walled sporocyst in Figure 4L could represent such a final stage.

Ultrastructure

Transmission electron microscopy (TEM) showed small zoites with alveoli- and rhoptry-like organelles in the lumen of digestive tubuli (Figure 5A,B). Infiltrating zoites seemed to induce local recruitment of microvilli enclosing them within the host epithelium (Figure 5C), or induce openings between epithelial cells, reaching the basal regions deeply within the digestive tubular cells (Figure 5D). Furthermore, we found an indication for sexual replication (gamogony) as two types of gamogonial stages were found within the digestive glands. A free small gamont-like cell without flagella (Figure 5E,F) and a large gamont-like cells containing an organelle with mitochondria-like morphology (Scholtyseck et al., 1972), developing within parasitophorous vacuoles (Figure 5G,H). The ultrastructure demonstrated the fusion of gametes, forming zygotes supporting anisogamogonial cell development as part of the lifecycle (Figure 5I). In semithin sections, signs of gamonts in similar formations adjacent to sporogonic formations were observed within parasitophorous vacuoles (Figure 5J,K).

Gamonts in zygote formation and sporozoites can form clusters of amylopectin granules (Valigurová & Koudela, 2006). Within electrondense vermozoite cells, we detected long clusters of amyloid-pectin-like granules arranged in a snowflake pattern, also infiltrated with rhoptry-like structures. The ultrastructure shows zygotes forming into oval semicircles and potentially spherical oocysts (Figure 5L–N). This could be the start of a sporogonial development with the formation of oocysts and sporocysts within digestive glands. Multiple electron lucent sporoblasts or immature oocysts (Figure 5O) were proliferating in large numbers primarily in the mussels collected in September, often enclosed within a vacuole. Within these, a few oocysts also developed inner electrondense sporocysts or enclosed sporozoites that appeared almost black under electron microscopy (Figure 5P).

Hypothetical life cycle

We compiled the result from histology, cytology, TEM, and ISH into a putative life cycle of lineage A within different organs and exit into the environment (Figure 6). Very few life cycle descriptions exist for gregarines in bivalves and all are based on marine hosts; we have used the description of *Nematopsis ostrearum* as support (Prytherch, 1940). To illustrate the anatomy of *M. margaritifera* and the spread via different organs we prepared a Figure S3 where anatomical characteristics are shown as line drawing (Figure S3A) and the corresponding composite image HE stained (Figure S3B). We hypothetize that cell infiltration begins within the epithelium of gills and mantle by infiltration of naked spores (gymnospores) where development starts (asexual replication), which then spreads throughout the host via hemolymph or circulating hemocytes (Figure 6.-6.5, Figure S3C). Further asexual division results in mono/di/polyzoic cysts that invade the connective tissue of different organs as histozoic cysts (Figure 6:6). Since only very few of these were detected embedded within the connective tissue of the digestive glands, the proliferation within digestive tubules is more likely distributed within the host as oral uptake. Zoites released from initial cell division in the gills and mantle (Figure 6:7, Figure S3D) are therefore the more likely transport route, leading cells into the stomach and further to the digestive gland via the digestive ducts (Figure 6:8, Figure S3E). These parasitic cells infiltrate the epithelia of the digestive cells (Figure S3F), where cell division continues. Pairing of zoites involving larger and smaller elongated cells in a syzygy-like position was observed within digestive tubuli (Figure 6:9, Figure S3G) supporting gamogonial development. The fusion of gametes into zygotes and further into sporulating cysts (oocysts), would

FIGURE 4 Histological sections of *Margaritifera margaritifera*, with morphological descriptions of gregarine cells within different organs. (A) Section of a hemocyte within mantel, where the nuclei is dislocated and the cytoplasm filled with multiple vacuoles, indicating infiltration or phagocytizing of multiple zoites. The vacuoles are highlighted with blue arrowhead (DIC image). (B) Hemocyte phagocytizing or releasing a folded zoite enclosed within a vacuole indicated with a blue arrowhead. (C) Early formation of gregarine cyst after infiltration of connective tissue within heart auricles (blue arrowhead). Adjacent, gymnospore-like cells, indicated with a white arrowhead. (D) Hemolymph compartment with development of multiple zoites enclosed within droplets (i.e. naked gregarine spores, gymnospores). (E) Thick-walled gregarine cyst within hemolymph compartment. A single basophilic zoite clearly seen within the cyst wall (blue arrowhead). (F) Histozoic gregarine spore formation, weakly basophilic, within the connective tissue of heart auricles. (G) Detaching spore/zoite, released from the epithelia layers of mantel. (H) Section of digestive gland with sporoblast formation attached to basophilic cell nuclei enclosed within a parasitophorous vacuole. Enclosed formations of internal cysts seen in the center of the sproblast (blue arrowhead, phase contrast). (I) Early oocyst development, partly enclosing internal sporocysts or immature sporozoite (blue arrowhead), phase contrast. (J) Digestive gland with one basophilic sporulated cyst enclosed within residual external membrane and still enclosed in a parasitic vacuole. Within the cyst, two folded sporozoites (darkly basophilic vermiform cells) can be seen. (K) Section of intestine revealing developing sporocysts with double layered soft cyst-wall (blue arrowhead). The same cell shown by phase contrast, white arrowhead. The larger cyst is unsporulated with signs of further separation into single sporocyst indicated by white arrow. (L) Large sporocyst enclosing single sporozoite. The external cystwall was refractile/weakly yellow visualized by phase contrast, indicating thick and rigid cystwall formation. This may indicate a fully sporulated cyst before being released as a fecal outlet.

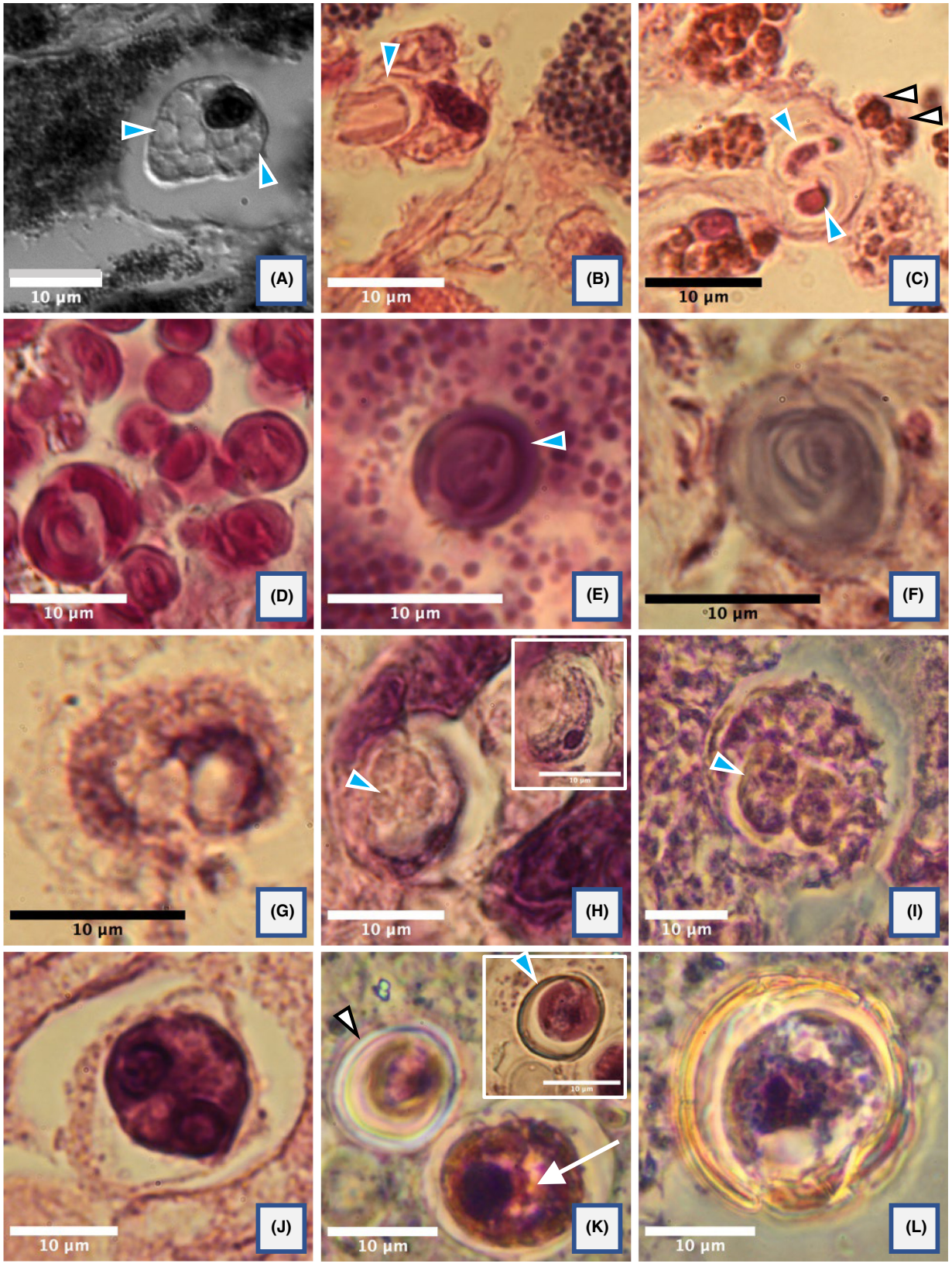

represent a sporogonic part of the lifecycle. Within the digestive gland, sporogony is likely the start of new proliferative cycles where fusing gametes produce sporoblasts. These developed further into immature oocysts that grow and expand in size, enclosing two or four sporocysts/sporozoites within the oocyst (Figure 6:10, Figure S3H), similar to descriptions of eugregarine sporogony in insects (Dias et al., 2017). In September, large numbers of parasitic

vacuoles were observed containing single to multiple unsporulated oocysts, which were shed via rupturing of the digestive gland epithelium. In the intestine, further maturation of unsporulated oocysts was observed, producing mono- or dizoic sporocysts (Figure S3I). However, the formation of different-sized sporocyst cells was puzzling, with smaller and possibly double overlapping elastic cystwalls (Figure 6:11, Figure S3J), and few examples of larger thick-walled refringent and dense cystwalls (Figure 6:12) indicating potentially two types of sporocysts. The final morphology with fully sporulated cysts is therefore still unclear.

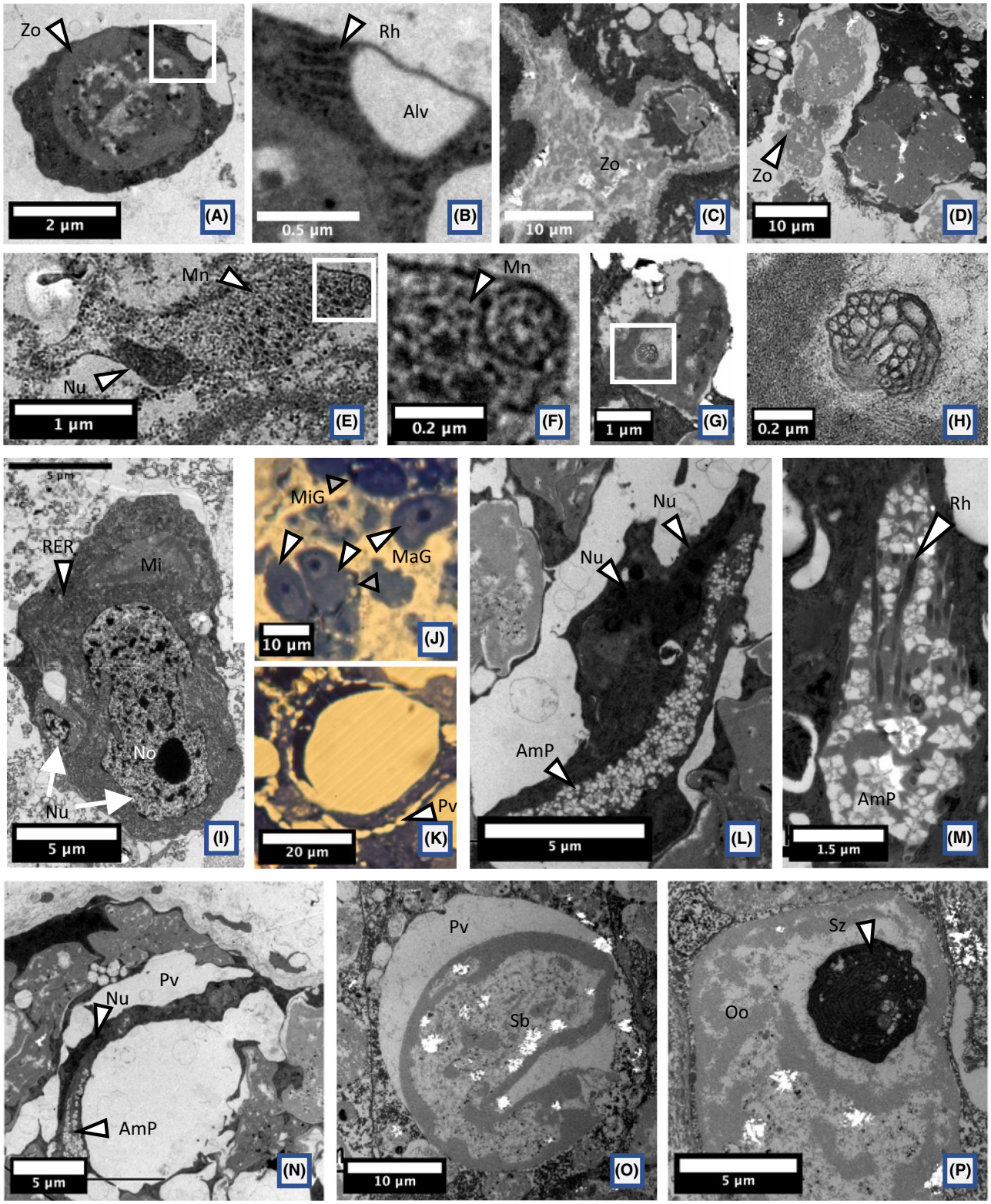

Journal of Eukaryotic Microbiology ISOP Published by the International Society of Protistologists

FIGURE 5 Ultrastructure of digestive gland with micrographs of putative gregarine infiltration and indication of gamogony and sporogony. (A and B) Free zoite within the lumen of tertiary digestive gland. Rhophtry and alveoli-like organelles indicated. (C) Infiltration of zoite enclosed by host microvilli. (D) Closely associated zoites with larger (electron lucent) and smaller (electron dense) cells arranged in a chain, reaching deep between the digestive gland epithelium. (E and F) Free small gamont-like cell, with mitochondria and microneme-like structures. (G and H) Large gamont-like cell within parasitophorous vacuole with clear mitochondria-like organelle in the center (enlarged in image H). (I) Fusion of a small and large gamont forming a zygote. Rough endoplasmatic reticulum dominating the cytoplasm. (J) multiple larger (white arrowhead) and smaller (gray arrowhead) gamonts. (K) Formation of a large parasitophorous vacuole, enclosing one dark blue sporozoite and one light blue sporoblast, and multiple vacuoles in the external rim (white arrowhead). (L) Zygote (electrondense) with the formation of amylopectin granules, arranged in a string with snowflake-like pattern. Fusion of nuclei indicated with arrowhead. (M) Close-up visualizing the amylopectin-like granules infiltrated with rhoptry-like organelles. (N) Formation of a parasitophorous vacuole enclosing a sporozoite forming into a closing circle. Note the nuclei and amylopectin-like granule indicated with white arrowheads. (O) Sporoblast (elecronlucent) enclosed within parasitophorous vacuole. (P) Oocyst (electron lucent) with formation of a sporozoite (electron dense) in cross-section. (J and K) Semithin sections, tuloidin stained. Alv, alveoli-like; AmP, amylopectin like granules; MaG, Macrogamont; MiG, Microgamont; Mn, microneme; Nu, nucleus; Oo, oocyst; Pv, parasitophorous vacuole; RER, ribosomal endoplasmatic reticulum; Rh, rhoptry-like; Sb, sporoblast; Sz, sporozoite; Zo, zoite. The size indicated by scalebar in each image.

DISCUSSION

We report the findings of novel diversity of gregarines associated with the highly endangered freshwater pearl mussel species *M. margaritifera* in Swedish streams. Two main new groups of related 18S rDNA sequences were obtained (Figure 1). One group (lineage A) is related to a described parasite in tadpoles, *Nematopsis temporariae*, and was found almost exclusively (with one exception – sequence accession number: OR168627) in association with individuals suffering mass mortality events (Figure 1, Figure S1 and Table S4). Five environmental sequences from lakes and permafrost soil also belong to this group. The other main group (lineage C) was only recovered from *M. margaritifera* collected in the reference population (Stommebäcken), which was not experiencing mass mortality at the time of sampling and did not show signs of a gregarine infection. Further efforts are needed to understand the nature of host interaction of these gregarine species on the spectrum of symbiosis (Rueckert et al., 2019). In addition to these two main groups, we also recovered in the MME population one sequence (lineage B), which is most closely related to the *N. temporariae* parasites found in tadpoles (Chambouvet et al., 2016).

The genus *Nematopsis* has long been known since the first morphological description of a parasitic infection in scallops in 1892 (Kinne & Lauckner, 1983). Many reports have since been published of cells attributed to *Nematopsis*, mainly in marine invertebrates such as crustaceans and bivalves, all based on morphological descriptions of gamogony and sporogony (bivalve hosts), and schizogony (crustacean hosts) (Abdel-Baki et al., 2012; Azevedo & Cachola, 1992; Chakraborti & Bandyopadhyay, 2010; Silva et al., 2019; Vivares, 1969). The *Nematopsis* species known to infect marine bivalves are characterized by monozoic, naked sporozoites within thick-walled cysts (Kinne & Lauckner, 1983). *Nematopsis* spp. is an exception among gregarines as they typically use two hosts to complete their lifecycle. Recent investigations indicated that the known host range of *Nematopsis* species also includes marine polychaetes (Morales-Covarrubias et al., 2014) and, unexpectedly, tadpoles in freshwater environment (Chambouvet et al., 2016).

The tadpole parasite (*N. temporariae*) is the first *Nematopsis* species with both morphology and molecular data available. However, the assignment of this parasite to *Nematopsis* and its phylogenetic placement in a terrestrial clade challenged previous taxonomy based on morphology, which has considered *Nematopsis* as part of the marine clade Porosporidae (Cavalier-Smith, 2014; Rueckert et al., 2011). This is further conflicting with a recent study placing *Porosporida gigantea* as a sister group to marine gregarine and not with *N. temporariae* (Boisard et al., 2022). Thus, it is currently uncertain whether *N. temporariae* and the new associated diversity we describe here are truly members of the genus *Nematopsis*. Clarification of the affiliation of these sequences will require obtaining molecular data for marine *Nematopsis*.

The possibility of a wrong assignment to *Nematopsis* of the tadpole parasite is substantiated by our microscopic investigations of the new parasitic diversity within *M. margaritifera*, which revealed some similarities but also key differences with published reports of marine *Nematopsis*. For example, clusters of cysts in gills containing single or multiple vermozoite-like cells (Figures 2 and 3) are similar to descriptions of *Nematopsis* cysts in marine bivalves such as scallops, blue mussels, and oysters (Kinne & Lauckner, 1983; Prytherch, 1940; Vivares, 1969). Within the digestive system, a few darkly eosinophilic cysts were detected (Figure 4J), again similar to cysts described in marine *Nematopsis* (Belafastova, 1996; Kinne & Lauckner, 1983; Prytherch, 1940; Silva et al., 2019; Tuntiwaranuruk et al., 2004; Vivares, 1969). This was also the case of the single sporozoite observed within monozoic sporocysts (Figure 4K–L), corresponding to be the final stage of *Nemotopsis* cyst formation in marine mollusks (Prytherch, 1940). However, all marine *Nematopsis* descriptions refer to histozoic cyst formation, enclosing cysts within connective tissue (Kinne & Lauckner, 1983; Silva et al., 2019; Tuntiwaranuruk et al., 2004; Vivares, 1969). Our observations partly support the presence of such histozoic cysts, but the ongoing oocyst release from the digestive gland and transformation into sporocysts later via intestine passage as fecal release (Figure 4K,L) do not correspond

to these descriptions. Furthermore, the transformation of oocysts into sporocysts enclosing double sporozoites and further separation into monozoic sporocysts differ from the descriptions of marine *Nematopsis* spp., where clusters or single gregarine always sporulates inside an organ without release. Description of the tadpole infection in the liver also indicates that these gregarine cysts are released from the host since only empty oocysts could

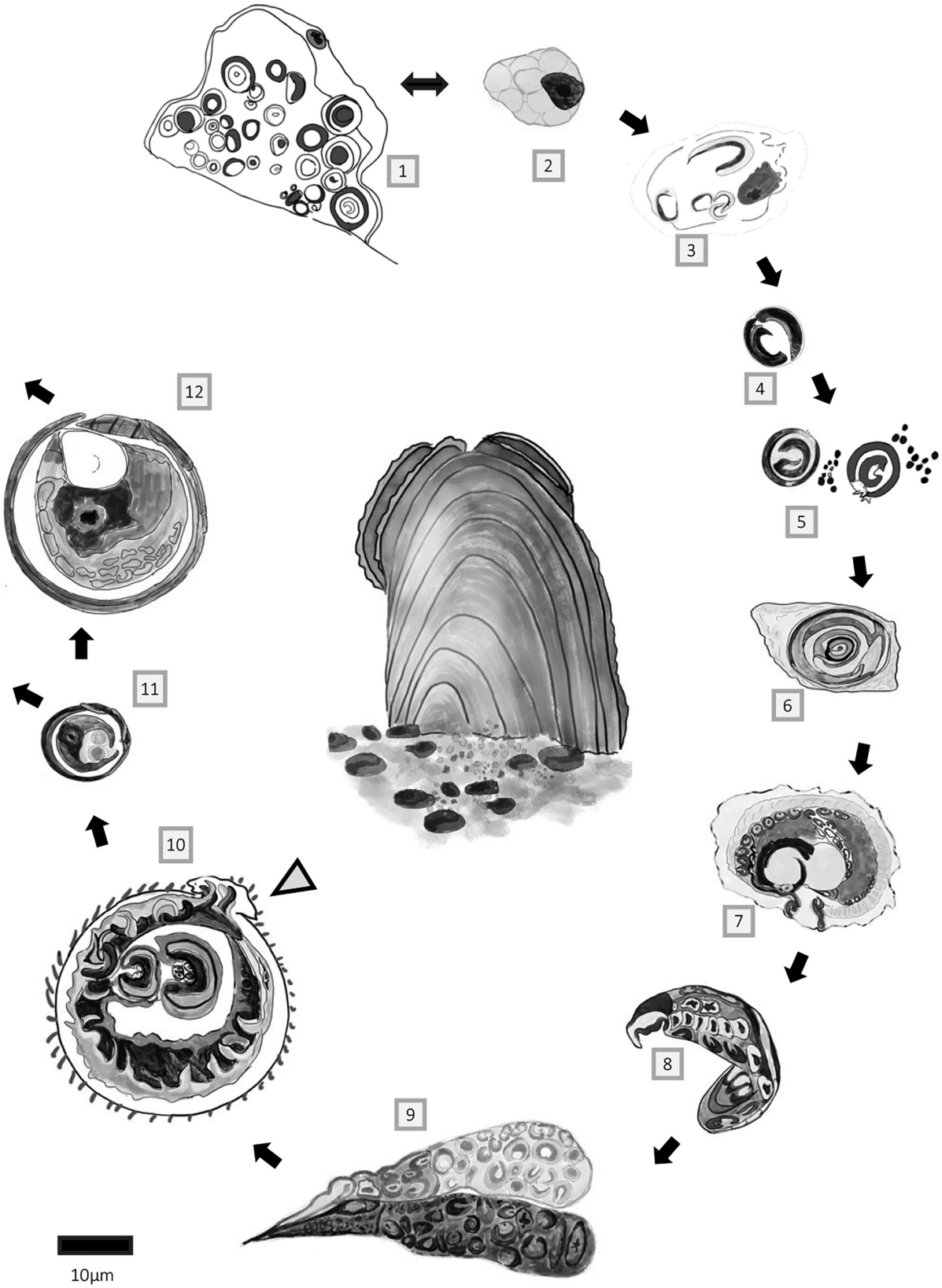

FIGURE 6 Hypothetical lifecycle of the new gregarine lineage A within the host *Margaritifera margaritifera* from Teåkersälven (MME population). (1) Sporozoites or gymnospores from the environment are proposed to infiltrate the gills and mantel via host feeding activity, for example, water filtration. Multiple zoites are shown expanding in size, attached to the gills and separating the epithelial layer from skeletal cells. (2) Hemocytes and phagocytizing cells expand in size when infiltrated by the parasite zoites, initially enclosed in vesicles. (3) Zoites are released from degenerative, rupturing host cells. (4) Free or enclosed zoites within hemolymph droplets. (5) Encapsulated thick-walled zoites dispersed throughout the hemolymph system. (6) Further cell division results in mono/di/polyzoic cysts, infiltrating connective tissue as histozoic cysts across different organs and probably dispersed throughout the hemolymph system, as free zoites or within circulating hemocytes. (7) Detachment of histozoic cysts within the mantel and gills, releasing zoites from rupturing host cell. (8) The released zoites are likely also transported as food particles to the stomach and into the digestive glands via the digestive ducts. (9) In the lumen of the digestive glands, the zoites attach and become confined within digestive vesicular cells. Paring of zoites involves larger elongated cells in syzygy-like position, observed within or escaping digestive tubuli cells. (10) Many spherical or encircled zoites were observed inside the digestive glands enclosed within a parasitophorous vacuoles. In some parasitophourous vacuoles, cysts were observed attached to the host, via an attachment disc (indicated with a gray arrowhead). (11) The fusion of gametes into zygotes and then into sporulating cysts (oocysts) may represent a sporogonic part of the lifecycle. Oocysts with elastic or thin walls were often observed within the lumen of the intestinal tract. (12) Very few mature oocysts were detected within the digestive glands, indicating delayed sporulation. Observations from the lumen support the fecal dispersal of oocysts since multiple mono- or dizoic oocysts were observed in the intestine. A few cysts displayed a very thick wall appearing almost crystalline. All life stages and cells are drawn to scale, size indicated by the scalebar. The image in the middle shows a freshwater pearl mussel in its normal filtrating position, halfway buried into the bottom sediments.

be recovered after the metamorphose phase, when tadpoles have transformed into subadult frogs (Chambouvet et al., 2016). These reported gregarine cysts within tadpole livers appear not thick-walled and thus do not fully correspond to the morphological descriptions of marine *Nematopsis* where the thick cyst wall is a defining feature of this genus (Kinne & Lauckner, 1983).

All known terrestrial eugregarine infections are monocyclic and are often restricted to the lumen of digestive system within the insect, normally attached to epithelial cells (Clopton, 2002). However, in some terrestrial eugregarines such as the ascogregarine infections of mosquitos, the parasites develop intracellularly within epithelia cells and are shed as oocysts via fecal release (Lantova & Volf, 2014), similar to the putative life cycle presented here (Figure 6). Other gregarine-related parasites infecting aquatic hosts, such as *Cryptosporidium* spp. found in fish, also exemplify intracellular cell development in which the sporogonial part takes place in parasitophorous vacuoles deeply nested within the cytoplasm of the epithelial cells. This is in contrast to all other cryptosporidians in vertebrates where development takes place in an apical position attached to the epithelial cells (Alvarez-Pellitero & Sitjà-Bobadilla, 2002; Couso-Pérez et al., 2022).

A lot remains to be understood about the novel gregarine diversity we report here and its interaction with *M. margaritifera*. Most importantly, the significance of the observed summer seasonality of lineage A in the mussel host is unclear, but could indicate that other hosts are involved in other parts of the years. This would be a novelty as all descriptions of terrestrial gregarines thus far support monoxeneus life cycles. An in-depth description of the life stages of the novel lineage C within *M. margaritifera*, and its impact on the host, also requires further investigations. Our work clearly reveals that gregarine parasites are found within the freshwater pearl mussels *M. margaritifera*, some associated with mass mortality of this ecologically critical species in streams and rivers. In the future, this knowledge should be taken into account in conservation efforts of this endangered species, for example when planning for relocation of populations and restocking attempts.

AUTHOR CONTRIBUTIONS

AA and FB designed the study. AA and NW performed field and sample collection. AA performed lab work. AA, IOB, NW, MJ, and AK analyzed data and prepared Figures. AA, IOB, FB, DP, AK, and MJ wrote and edited the paper.

ACKNOWLEDGMENTS

This research was supported by SciLifeLab, a Formas Future Research Leader grant (2017-01197), and a Swedish Research Council VR research project grant (2017-04563) all available to FB. We are thankful to Västra Götaland County, Dalslands miljö och energiförbund, and the Swedish Agency for Marine and Water Management for funding the collection and preparation of freshwater pearl mussels. We thank Ulrika Larsson Pettersson at the Department of Pathology and Wildlife (Swedish National Veterinary Institute) for assistance with ISH, and Karin Staxäng at the Biovis platform (Uppsala University) for TEM-preparation and guidance in TEM imaging. Finally, we are grateful to Mark Freeman at Ross University School of Veterinary Medicine (West Indies) for help with the ISH probe design. Computational analyses were enabled by resources in projects SNIC2021/5-302, SNIC2021/22-178, NAISS2023-6-81and NAISS2023-5-122 provided by the Swedish National Infrastructure for Computing (SNIC) at UPPMAX, partially funded by the Swedish Research Council through grant agreement number 2018-0597.

ORCID

Anders Alfjorden https://orcid.org/0000-0003-1733-4085
Fabien Burki https://orcid.org/0000-0002-8248-8462

REFERENCES

Abdel-Baki, A.-A.S., Al-Quraishy, S., Dkhil, M.A., Al Nasr, I., Oliveira, E., Casal, G. et al. (2012) Ultrastructural characteristics

of *Nematopsis* sp. oocysts (Apicomplexa: Porosporidae), a parasite of the clam *Meretrix meretrix* (Veneridae) from the Arabian gulf, Saudi Arabia. *Folia Parasitologica*, 59(2), 81–86. Available from: https://doi.org/10.14411/fp.2012.012

Aldridge, D.C., Ollard, I.S., Bespalaya, Y.V., Bolotov, I.N., Douda, K., Geist, J. et al. (2023) Freshwater mussel conservation: a global horizon scan of emerging threats and opportunities. *Global Change Biology*, 29(3), 575–589. Available from: https://doi.org/10.1111/gcb.16510

Altschul, S.F., Gish, W., Miller, W., Myers, E.W. & Lipman, D.J. (1990) Basic local alignment search tool. *Journal of Molecular Biology*, 215(3), 403–410. Available from: https://doi.org/10.1016/S0022-2836(05)80360-2

Alvarez-Pellitero, P. & Sitjà-Bobadilla, A. (2002) *Cryptosporidium molnari* n. sp. (Apicomplexa: Cryptosporidiidae) infecting two marine fish species, *Sparus aurata* L. & *Dicentrarchus labrax*. *International Journal for Parasitology*, 32, 1007–1021.

Annenkova, N.V., Giner, C.R. & Logares, R. (2020) Tracing the origin of planktonic protists in an ancient lake. *Microorganisms*, 8, 543. Available from: https://doi.org/10.3390/microorganisms8040543

Azevedo, C. & Cachola, R. (1992) Fine structure of the Apicomplexa oocyst of *Nematopsis* sp. of two marine bivalve molluscs'. *Diseases of Aquatic Organisms*, 14, 69–73. Available from: https://doi.org/10.3354/dao014069

Azevedo, C. & Padovan, I. (2004) *Nematopsis gigas* n. sp. (Apicomplexa), a parasite of *Nerita Ascencionis* (Gastropoda, Neritidae) from Brazil. *Journal of Eukaryotic Microbiology*, 51(2), 214–219.

Belafastova, I. (1996) Gregarines of the genus *Nematopsis* (Eugregarinida, Porosporidae) -parasites of the Black Sea invertebrates. *Parazitologiya*, 30, 159–173.

Bates, S.T., Clemente, J.C., Flores, G.E., Walters, W.A., Wegener Parfrey, L., Knight, R. et al. (2013) Global biogeography of highly diverse protistan communities in soil. *ISME Journal*, 7(3), 652–659. Available from: https://doi.org/10.1038/ismej.2012.147

Berrilli, F., Ceschia, G., De Liberato, C., Di Cave, D. & Orecchia, P. (2000) Parasitic infections of *Chamelea gallina* (Mollusca, Bivalvia) from commercially exploited banks of the Adriatic Sea. *Bulletin of the European Association of Fish Pathologists*, 20(5), 199–205.

Boisard, J., Duvernois-Berthet, E., Duval, L., Schrével, J., Guillou, L., Labat, A. et al. (2022) Marine gregarine genomes reveal the breadth of apicomplexan diversity with a partially conserved glideosome machinery. *BMC Genomics*, 23(1), 1–22. Available from: https://doi.org/10.1186/s12864-022-08700-8

Bower, S.M., Carnegie, R.B., Goh, B., Jones, S.R.M., Lowe, G.J. & Mak, M.W.S. (2004) Preferential PCR amplification of parasitic protistan small subunit rDNA from metazoan tissues. *Journal of Eukaryotic Microbiology*, 51(3), 325–332. Available from: https://doi.org/10.1111/j.1550-7408.2004.tb00574.x

Bower, S.M., Hervio, D. & Meyer, G.R. (1997) Infectivity of *Mikrocytos mackini*, the causative agent of Denman Island disease in Pacific oysters *Crassostrea gigas*, to various species of oysters'. *Diseases of Aquatic Organisms*, 29(2), 111–116. Available from: https://doi.org/10.3354/dao029111

Callahan, B.J., McMurdie, P.J., Rosen, M.J., Han, A.W., Johnson, A.J.A. & Holmes, S.P. (2016) DADA2: high-resolution sample inference from illumina amplicon data. *Nature Methods*, 13(7), 581–583. Available from: https://doi.org/10.1038/nmeth.3869

Capella-Gutiérrez, S., Silla-Martínez, J.M. & Gabaldón, T. (2009) TrimAl: a tool for automated alignment trimming in large-scale phylogenetic analyses'. *Bioinformatics*, 25(15), 1972–1973. Available from: https://doi.org/10.1093/bioinformatics/btp348

Carnegie, R.B., Meyer, G.R., Blackbourn, J., Cochennec-Laureau, N., Berthe, F.C.J. & Bower, S.M. (2003) Molecular detection of the oyster parasite *Mikrocytos mackini*, and a preliminary phylogenetic analysis. *Diseases of Aquatic Organisms*, 54(3), 219–227. Available from: https://doi.org/10.3354/dao054219

Carrasco, N., Green, T. & Itoh, N. (2015) *Marteilia* spp. parasites in bivalves: a revision of recent studies. *Journal of Invertebrate Pathology*, 131, 43–57. Available from: https://doi.org/10.1016/j.jip.2015.07.016

Cavalier-Smith, T. (2014) Gregarine site-heterogeneous 18S rDNA trees, revision of gregarine higher classification and the evolutionary diversification of sporozoa. *European Journal of Protistology*, 50(5), 472–495. Available from: https://doi.org/10.1016/j.ejop.2014.07.002

Chakraborti, J. & Bandyopadhyay, P.K. (2010) First record of a parasitic septate gregarines (Apicomplexa: Sporozoea) in the shrimp *Peneaus monodon* in Sundarbans of West Bengal. *Journal of Parasitic Diseases*, 34(1), 40–43. Available from: https://doi.org/10.1007/s12639-010-0002-7

Chambouvet, A., Valigurová, A., Pinheiro, L.M., Richards, T.A. & Jirků, M. (2016) *Nematopsis temporariae* (Gregarinasina, Apicomplexa, Alveolata) is an intracellular infectious agent of tadpole livers. *Environmental Microbiology Reports*, 8(5), 675–679. Available from: https://doi.org/10.1111/1758-2229.12421

Čižmek, H., Čolić, B., Gračan, R., Grau, A. & Catanese, G. (2020) An emergency situation for pen shells in the Mediterranean: the Adriatic Sea, one of the last *Pinna nobilis* shelters, is now affected by a mass mortality event. *Journal of Invertebrate Pathology*, 173(October), 107388. Available from: https://doi.org/10.1016/j.jip.2020.107388

Clopton, R.E. (2002) The gregarines: a generic level review. In: Leedale, G., Lee, Patterson, D. & Bradbury, P.C. (Eds.) *Illustrated guide to the protozoa*, 2nd edition. Lawrence, KS: Society of Protzoologists, pp. 1–58.

Clopton, R.E. (2009) Phylogenetic relationships, evolution and systematic revision of the septate gregarines (Apicomplexa: Eugregarinorida: Septatorina). *Comparative Parasitology*, 76(2), 167–190. Available from: https://doi.org/10.1654/4388.1

Clopton, R.E., Cook, T.J. & Cook, J.L. (2007) Revision of *Geneiorhynchus* Schneider, 1875 (Apicomplexa: Eugregarinida: Actinocephalidae: Acanthosporinae) with recognition of four new species of *Geneiorhynchus* and description of *Geneiorhynchus manifestus* n. sp. parasitizing naiads of the Green Darner. *Comparative Parasitology*, 74(2), 273–285. Available from: https://doi.org/10.1654/4286.1

Couso-Pérez, S., Ares-Mazás, E. & Gómez-Couso, H. (2022) A review of the current status of cryptosporidium in fish. *Parasitology*, 149(4), 444–456. Available from: https://doi.org/10.1017/S0031182022000099

Cruaud, P., Vigneron, A., Fradette, M.-S., Dorea, C.C., Culley, A.I., Rodriguez, M.J. et al. (2019) Annual protist community dynamics in a freshwater ecosystem undergoing contrasted climatic conditions: the Saint-Charles River (Canada). *Frontiers in Microbiology*, 10(October), 2359. Available from: https://doi.org/10.3389/fmicb.2019.02359

De Vargas, C., Audic, S., Henry, N., Decelle, J., Mahé, F., Logares, R. et al. (2015) Eukaryotic plankton diversity in the sunlit ocean. *Science*, 348(6237), 1261605. Available from: https://doi.org/10.1007/s13398-014-0173-7.2

Del Campo, J., Pons, M.J., Herranz, M., Wakeman, K.C., Del Valle, J., Vermeij, M.J.A. et al. (2019) Validation of a universal set of primers to study animal-associated microeukaryotic communities. *Environmental Microbiology*, 21, 3855–3861. Available from: https://doi.org/10.1111/1462-2920.14733

Dias, G., Dallai, R., Carapelli, A., Almeida, J.P.P., Campos, L.A.O., Faroni, L.R.A. et al. (2017) First record of gregarines (Apicomplexa) in seminal vesicle of insect. *Scientific Reports*, 7(1), 1–9. Available from: https://doi.org/10.1038/s41598-017-00289-3

Haag, W.R. (2019) Reaessing enigmatic mussel declines i the United States. *Freshwater Mollusk Biology and Conservation*, 22, 43–60. Available from: https://doi.org/10.31931/fmbc.v22i2.2019.43-60

Hatt, P. (1931) L'evolution des porosporides ches les mollusc. *Archives Zoological Exploration of Genus*, 72, 341–415.

Henrikson, l. & Söderberg, H. (2020) Åtgärdsprogram för flodpärlmussla *Margaritifera margaritifera* (Linnaeus, 1758). Available from: https://www.havochvatten.se/data-kartor-och-rapporter/rapporter-och-andra-publikationer/publikationer/2020-05-29-atgardsprogram-for-flodparlmussla.html

Howard, D.W. & Smith, C.S. (1983) Histological Techniques for marine bivalve mollusks. U.S. Department of Service, National Oceanic and Atmospheric Administration, National Marine Fisheries Service. NOAA Technical Memorandum NMFS-F/NEC-25, June: 1–97.

Huse, S.M., Welch, D.B.M., Voorhis, A., Shipunova, A., Morrison, H.G., Eren, A.M. et al. (2014) VAMPS: a website for visualization and analysis of microbial population structures. *BMC Bioinformatics*, 15(1), 41. Available from: https://doi.org/10.1186/1471-2105-15-41

Iritani, D., Banks, J.C., Webb, S.C., Fidler, A., Horiguchi, T. & Wakeman, K.C. (2021) New gregarine species (Apicomplexa) from tunicates show an evolutionary history of host switching and suggest a problem with the systematics of Lankesteria and Lecudina. *Journal of Invertebrate Pathology*, 183, 107622. Available from: https://doi.org/10.1016/j.jip.2021.107622

Jamy, M., Biwer, C., Vaulot, D., Obiol, A., Jing, H., Peura, S. et al. (2022) Global patterns and rates of habitat transitions across the eukaryotic tree of life. *Nature Ecology & Evolution*, 6(10), 1458–1470. Available from: https://doi.org/10.1038/s41559-022-01838-4

Kearse, M., Moir, R., Wilson, A., Stones-Havas, S., Cheung, M., Sturrock, S. et al. (2012) Geneious basic: an integrated and extendable desktop software platform for the organization and analysis of sequence data. *Bioinformatics*, 28(12), 1647–1649. Available from: https://doi.org/10.1093/bioinformatics/bts199

Khomich, M., Kauserud, H., Logares, R., Rasconi, S. & Andersen, T. (2017) Planktonic protistan communities in lakes along a large-scale environmental gradient. *FEMS Microbiology Ecology*, 93(4), 231. Available from: https://doi.org/10.1093/femsec/fiw231

Kinne, O. & Lauckner, G. (1983) *Diseases of marine animals, Volume 2: Introduction, Bivalvia to scaphopoda. Biologishe Anstalt Helgoland*, Vol. 2. Hamburg: Biologishe Anstalt Helgoland. Available from: https://doi.org/10.1016/0198-0149(81)90045-5

Kristmundsson, Á. & Freeman, M.A. (2018) Harmless sea snail parasite causes mass mortalities in numerous commercial scallop populations in the northern hemisphere. *Scientific Reports*, 8(1), 1–12. Available from: https://doi.org/10.1038/s41598-018-26158-1

Lantova, L. & Volf, P. (2014) Mosquito and sand fly gregarines of the genus *Ascogregarina* and *Psychodiella* (Apicomplexa: Eugregarinorida, Aseptatorina) – overview of their taxonomy, life cycle, host specificity and pathogenicity. *Infection, Genetics and Evolution*, 28, 616–627. Available from: https://doi.org/10.1016/j.meegid.2014.04.021

Leander, B.S. (2008) Marine gregarines: evolutionary prelude to the apicomplexan radiation? *Trends in Parasitology*, 24(2), 60–67. Available from: https://doi.org/10.1016/j.pt.2007.11.005

Mahé, F., De Vargas, C., Bass, D., Czech, L., Stamatakis, A., Lara, E. et al. (2017) Parasites dominate hyperdiverse soil protist communities in neotropical rainforests. *Nature Ecology & Evolution*, 1(4), 0091. Available from: https://doi.org/10.1038/s41559-017-0091

Minh, B.Q., Schmidt, H.A., Chernomor, O., Schrempf, D., Woodhams, M.D., Von Haeseler, A. et al. (2020) IQ-TREE 2: new models and efficient methods for phylogenetic inference in the genomic era. *Molecular Biology and Evolution*, 37(5), 1530–1534. Available from: https://doi.org/10.1093/molbev/msaa015

Moorkens, E., Cordeiro, J., Seddon, M.B., von Proschwitz, T. & Woolnoug, T. (2017) *Margaritifera margaritifera* (errata version published in 2018). The IUCN Red List of threatened species 2017: E.T12799A128686456. 2017. https://doi.org/10.2305/IUCN.UK.2017-3.RLTS.T12799A508865.en

Morales-Covarrubias, M.S., Cuellar-Anjel, J., Pantoja, C., Lightner, D.V., Gomez, B., Barracco, M.A. et al. (2014) In: Morales, V. & Cuellar-Angel, J. (Eds.) *Patologia e inmunologia de camarones penaeidos*, 2nd edition. OIRSA, Panama: New Concept Publication Inc.

Peura, S., Wauthy, M., Simone, D., Eiler, A., Einarsdóttir, K., Rautio, M. et al. (2020) Ontogenic succession of thermokarst thaw ponds is linked to dissolved organic matter quality and microbial degradation potential. *Limnology and Oceanography*, 65(S1), S248–S263. Available from: https://doi.org/10.1002/lno.11349

Prytherch, H.F. (1940) The life cycle and morphology of *Nematopsis ostrearum*, sp. nov. a gregarine parasite of the mud crab and oyster. *Journal of Morphology*, 66(1), 39–65. Available from: https://doi.org/10.1002/jmor.1050660106

Richard, J.C., Leis, E., Dunn, C.D., Agbalog, R., Waller, D., Knowles, S. et al. (2020) Mass mortality in freshwater mussels (*Actinonaias pectorosa*) in the Clinch River, USA, linked to a novel Densovirus. *Scientific Reports*, 10(1), 1–11. Available from: https://doi.org/10.1038/s41598-020-71459-z

Rozewicki, J., Li, S., Amada, K.M., Standley, D.M. & Katoh, K. (2019) MAFFT-DASH: integrated protein sequence and structural alignment. *Nucleic Acids Research*, 47(W1), W5–W10. Available from: https://doi.org/10.1093/nar/gkz342

Rueckert, S., Betts, E.L. & Tsaousis, A.D. (2019) The symbiotic spectrum: where do the gregarines fit? *Trends in Parasitology*, 35(9), 687–694. Available from: https://doi.org/10.1016/j.pt.2019.06.013

Rueckert, S., Simdyanov, T.G., Aleoshin, V.V. & Leander, B.S. (2011) Identification of a divergent environmental DNA sequence clade using the phylogeny of gregarine parasites (Apicomplexa) from crustacean hosts. *PLoS One*, 6(3), e18163. Available from: https://doi.org/10.1371/journal.pone.0018163

Scholtyseck, E., Mehlhorn, E.H. & Hammond, D.M. (1972) Electron microscope studies of microgamteogenesis in coccidia and related groups. *Zeitschrift Fur Parasitenkunde*, 38(2), 95–131.

Seppey, C.V.W., Broennimann, O., Buri, A., Yashiro, E., Pinto-Figueroa, E., Singer, D. et al. (2020) Soil protist diversity in the swiss western alps is better predicted by topo-climatic than by edaphic variables'. *Journal of Biogeography*, 47(4), 866–878. Available from: https://doi.org/10.1111/jbi.13755

Silva, T.J., Soares, E.C., Casal, G., Rocha, S., Santos, E.L., Nascimento, R. et al. (2019) Ultrastructure of phagocytes and oocysts of *Nematopsis* sp. (Apicomplexa, Porosporidae) infecting *Crassostrea rhizophorae* in northeastern Brazil. *Revista Brasileira de Parasitologia Veterinária*, 28(1), 97–104. Available from: https://doi.org/10.1590/s1984-29612019010

Singer, D., Duckert, C., Heděnec, P., Lara, E., Hiltbrunner, E. & Mitchell, E.A.D. (2020) High-throughput sequencing of litter and moss eDNA reveals a positive correlation between the diversity of Apicomplexa and their invertebrate hosts across alpine habitats'. *Soil Biology and Biochemistry*, 147(April), 18–21. Available from: https://doi.org/10.1016/j.soilbio.2020.107837

Smith, A.J. & Cook, T.J. (2012) Revision of the genus Prismatospora and description of *Prismatospora cloptoni* n. sp. (Apicomplexa: Actinocephalidae: Acanthosporinae) from Naiads of the Green Darner, *Anax junius* (Odonata: Anisoptera: Aeshnidae), in East Texas, U.S.A. *Comparative Parasitology*, 79(1), 9–14. Available from: https://doi.org/10.1654/4527.1

Smith-Herron, A.J. (2015) *Hoplorhynchus aster* n. sp. (Apicomplexa: Actinocephalidae: Menosporinae) and *Anguilloforma marcelyni* gen. et n. sp. (Apicomplexa: Actinocephalidae: Acanthosporinae) infecting *Ischnura ramburii* and *Enallagma civile* (Zygoptera: Coenagrionidae) from Texas, USA. *Comparative Parasitology*, 82(2), 211–218. Available from: https://doi.org/10.1654/4763.1

Tseng, M. (2007) Ascogregarine parasites as possible biocontrol agents of mosquitoes. *Journal of the American Mosquito Control Association*, 23(2 Suppl), 30–34. Available from: https://doi.org/10.2987/8756-971x(2007)23[30:apapba]2.0.co;2

Tuntiwaranuruk, C., Chalermwat, K., Upatham, E.S., Kruatrachue, M. & Azevedo, C. (2004) Investigation of *Nematopsis* spp. oocysts in 7 species of bivalves from Chonburi province, gulf of

Thailand. *Diseases of Aquatic Organisms*, 58(1), 47–53. Available from: https://doi.org/10.3354/dao058047

Valigurová, A. & Koudela, B. (2006) Ultrastructural study of developmental stages of *Mattesia dispora* (Neogregarinorida: Lipotrophidae), a parasite of the flour moth *Ephestia kuehniella* (lepidoptera). *European Journal of Protistology*, 42(4), 313–323. Available from: https://doi.org/10.1016/j.ejop.2006.07.007

Vivares, C.P. (1969) Etude du parasitisme des crustaces decapodes brachyoures en Mediterranee Occidentale. University de Montpellier, France.

von Proschwitz, T. & Wengström, N. (2021) Zoogeography, ecology and conservation status of the large freshwater mussels in Sweden. *Hydrobiologia*, 848(12–13), 2869–2890. Available from: https://doi.org/10.1007/s10750-020-04351-6

Wakeman, K.C. (2020) Molecular phylogeny of marine gregarines (Apicomplexa) from the Sea of Japan and the Northwest Pacific including the description of three novel species of *Selenidium* and *Trollidium akkeshiense* n. gen. n. sp. *Protist*, 171(1), 125710. Available from: https://doi.org/10.1016/j.protis.2019.125710

Wakeman, K.C. & Leander, B.S. (2013) Identity of environmental DNA sequences using descriptions of four novel marine gregarine parasites, *Polyplicarium* n. gen. (Apicomplexa), from capitellid polychaetes. *Marine Biodiversity*, 43(2), 133–147. Available from: https://doi.org/10.1007/s12526-012-0140-5

Wengström, N., Söderberg, H., Höjesjö, J. & Alfjorden, A. (2019) Mass mortality events in freshwater pearl mussel (*Margaritifera margaritifera*) populations in Sweden: an overview and indication of possible causes. *Freshwater Mollusk Biology and Conservation*, 22(2), 61. Available from: https://doi.org/10.31931/fmbc.v22i2.2019.61-69

Westling, A., Toräng, P., Jacobson, A., Halding, M. & Naeslund, M. (2020) Sveriges arter och naturtyper i EU:s art- och habitatdirektiv. Resultat från rapportering 2019 till EU av bevarandestatus 2013–2018. Bromma. Available from: https://www.artdatabanken.se/publikationer/beställ-publikationer/arter-och-naturtyper-i-eus-art-och-habitatdirektiv/

SUPPORTING INFORMATION

Additional supporting information can be found online in the Supporting Information section at the end of this article.

How to cite this article: Alfjorden, A., Onut-Brännström, I., Wengström, N., Kristmundsson, A., Jamy, M., Persson, B.D. et al. (2024) Identification of a new gregarine parasite associated with mass mortality events of freshwater pearl mussels (*Margaritifera margaritifera*) in Sweden. *Journal of Eukaryotic Microbiology*, 71, e13021. Available from: https://doi.org/10.1111/jeu.13021